Correspondence

Decentralized Nonlinear Adaptive Control of an HVAC System

Zhang Huaguang and Lilong Cai

***Abstract*—This correspondence presents a new decentralized nonlinear adaptive controller (DNAC) for a heating, ventilating, and air conditioning (HVAC) system capable of maintaining comfortable conditions under varying thermal loads. In this scheme, an HVAC system is considered to be two subsystems and controlled independently. The interactions between the two subsystems are treated as deterministic types of uncertain disturbances and their magnitudes are supposed to be bounded by absolute value. The decentralized nonlinear adaptive controller (DNAC) consists of an inner loop and an outer loop. The inner loop is a single-input fuzzy logic controller (FLC), which is used as the feedback controller to overcome random instant disturbances. The outer loop is a Fourier integral-based control, which is used as the frequency-domain adaptive compensator to overcome steady, lasting uncertain disturbances.**

The global DNAC controller ensures that the system output vector tracks a desired trajectory vector within the system bandwidth and that the tracking error vector converges uniformly to a zero vector. The simulated experimental results on the HVAC system show that the performance is dramatically improved.

***Index Terms*—Decentralized nonlinear adaptive control, Fourier integral, single-input FLC.**

NOMENCLATURE

h_w	Enthalpy of liquid water.
W_o	Humidity ratio of outdoor air.
h_v	Enthalpy of water vapor.
V_e	Volume of heat exchanger.
W_s	Humidity ratio of supply air.
C_p	Specific heat of air.
T_o	Temperature of outdoor air.
T_{ow}	Wet bulb temperature of outdoor air.
M_o	Moisture load.
Q_o	Sensible heat load.
V_s	Volume of thermal space.
ρ	Air mass density.
f	Volumetric flow rate of air (ft^3/min).
gpm	Flow rate of chilled water (gal/min).
T_2	Temperature of supply air.
T_{2w}	Wet bulb temperature of supply air.
T_3	Temperature of thermal space.
T_{3w}	Wet bulb temperature of thermal space.
W_3	Humidity ratio of thermal space.

Manuscript received June 17, 2000; revised September 30, 2001, and December 27, 2001. This work was supported by the National Natural Science Foundation (60274017) and the Specialized Research Fund for the Doctoral Program of Higher Education Foundation (2001045023) China, as well as a grant from the Research Grants Council of the Hong Kong Special Administrative Region, China (HKUST6192/01E).

Z. Huaguang is with the Department of Automatic Control, Northeastern University, Shenyang, 110006, China.

L. Cai is with the Department of Mechanical Engineering, Hong Kong University of Science and Technology, Clear Water Bay, Kowloon, Hong Kong.

Digital Object Identifier 10.1109/TSMCC.2002.807271

I. INTRODUCTION

The consumption of energy by heating, ventilating, and air conditioning (HVAC) equipment in commercial and industrial buildings constitutes 50% of the world energy consumption [6]. In spite of the advancements made in computer technology and its impact on the development of new control methodologies for HVAC systems aiming at improving their energy efficiencies, the process of operating HVAC equipment in commercial and industrial buildings is still an low-efficient and high-energy consumption process [8], [10]. Classical HVAC control techniques such as ON/OFF controllers (thermostats) and proportional-integral-derivative (PID) controllers are still very popular because of their low cost. However, in the long run, these controllers are expensive because they operate at a very low energy efficiency and fail to consider the complex nonlinear characteristics of the multi-input multi-output (MIMO) HVAC systems and the strong coupling actions between them.

In this correspondence, a decentralized nonlinear adaptive controller (DNAC) is used to control the HVAC systems. As we know decentralized control is an important control scheme for large-scale, complex systems. Researchers have done a large amount of work to improve the decentralized control scheme. A decentralized model reference adaptive control scheme is developed in [9], in which the relative degree can be greater than 2, but the structure of the controlled process and the nominal relative degree have to be known. A linear quadratic regulator theory to develop a decentralized robust controller for interconnected uncertain power systems is presented in [7], but only a linear controller is obtained. These schemes are usually formed in a time domain and is difficult to remove high frequency noises, measuring errors, and time-variant lasting uncertain disturbances in industrial plants. In order to solve these puzzle problems we propose the DNAC control scheme which has proven to be very suitable to apply to a variable air volume HVAC system capable of maintaining comfortable conditions within a thermal space with time-variant thermal loads acting upon the system. The proposed DNAC controller consists of a fuzzy feedback control (SFLC) and a frequency-domain adaptive compensator (FDAC), as presented in Fig. 1.

This correspondence is organized as follows. In Section II, we give a general description and some assumptions for a nonlinear HVAC system. Then, the SFLC feedback control law and its stability condition are presented in Section III. In Section IV, the design details of the FDAC compensator using the Fourier integral are given and the convergent conditions of the closed-loop DNAC system are provided. In Section V, the proposed DNAC method is used to control a nonlinear HVAC system and demonstrate the satisfactory performance of the proposed control system. Finally, Section VI presents the conclusion.

II. SYSTEM COMPONENTS AND DESCRIPTION

We consider the single-zone HVAC system described in [1]. In our discussion, we assume the system is operating on the cooling mode (air conditioning).

The controller maintains the thermal space temperature and humidity at the setpoints of 71 °F, and 55% relative humidity (RH), respectively. The control inputs for the system are the flow rate of cold water from the chiller to the heat exchanger and the circulating air flow rate using the variable speed fan. The main work processes of the system in the cooling mode are the same as that described in [1].

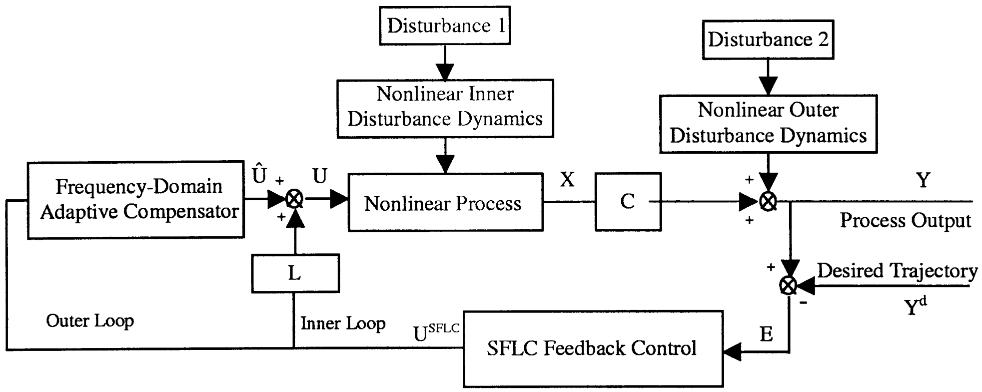

Fig. 1. Structure diagram of the DNAC.

Our objective is to design an HVAC control system aiming at maintaining comfortable conditions within a thermal space without energy waste. The importance of the problem at hand lies on the impact that energy efficient HVAC systems can have on commercial and industrial energy consumption.

A. HVAC Model

The state equations describing the dynamic behavior of the HVAC system are given by [1]

$$\dot{x}_1 = u_1\alpha_1 60(W_s - x_1) + \alpha_4 M_0 \quad (1)$$

$$\dot{x}_2 = u_1\alpha_1 60(x_3 - x_2) - u_1\alpha_2 60(W_s - x_1) + \alpha_3(Q_0 - h_v M_0) \quad (2)$$

$$\dot{x}_3 = u_1\beta_1 60(x_2 - x_3) + u_1 15\beta_1(T_0 - x_2) - u_1\beta_3 60((0.25W_0 + 0.75x_1) - W_s) - 100u_2\beta_2 \quad (3)$$

$$y_1 = x_1 \quad (4)$$

$$y_2 = x_2 \quad (5)$$

where

$$u_1 = f,\ u_2 = gpm,\ x_1 = W_3,\ x_2 = T_3,\ x_3 = T_2$$
$$y_1 = W_3,\ y_2 = T_3$$
$$\alpha_1 = \frac{1}{V_s}\ \ \alpha_2 = \frac{h_v}{C_p V_s}\ \ \alpha_3 = \frac{1}{\rho C_p V_s}$$
$$\beta_2 = \frac{1}{\rho C_p V_e}$$
$$\alpha_4 = \frac{1}{\rho V_s}\ \ \beta_1 = \frac{1}{V_e}\ \text{and}$$
$$\beta_3 = \frac{h_w}{C_p V_e}.$$

B. A General MIMO Nonlinear System Description

Without losing generality, the above HVAC model can be generalized as a class of interconnected MIMO system that consists of m dynamical subsystems. The pth subsystem is described as

$$x_p^{(n_p)} = f_p(\mathbf{X}_p,t) + g_p(\mathbf{X}_p,t)u_p(t) + \sum_{j=1}^{m}[fd_j(\mathbf{X}_j,t) + gd_j(\mathbf{X}_j,t)u_j(t)] + F_{p1}(t),$$
$$= f_p(\mathbf{X}_p,t) + g_p(\mathbf{X}_p,t)u_p(t) + d_{p1}(\chi,t) \quad (6)$$

$$y_p(t) = C_p x_p + d_{p2}(t), \quad p = 1,2,\ldots,m \quad (7)$$

with

$$\mathbf{X}_p = (x_{p1}, x_{p2}, \ldots, x_{pn_p})^T = \left(x_p, \dot{x}_p, \ldots, x_p^{(n_p-1)}\right)^T \quad (8)$$

$$d_{p1}(\chi,t) = F_{p1}(t) + \sum_{j=1}^{m}[fd_j(\mathbf{X}_j,t) + gd_j(\mathbf{X}_j,t)u_j(t)] \quad (9)$$

where $f_p(\mathbf{X}_p,t)$, $fd_j(\mathbf{X}_j,t)$, $g_p(\mathbf{X}_p,t)$, and $gd_j(\mathbf{X}_j,t)$ are unknown continuous functions representing the system dynamics; $F_{p1}(t)$ is the unknown internal disturbance, $d_{p2}(t)$ is the unknown external disturbance, $\mathbf{X}_p(t) \in R^{n_p}$ is the state vector of the pth subsystem, $u_p(t) \in R$ and $y_p(t) \in R$ are the input and output of the pth subsystem, respectively, $C_p \in R$ is a coefficient; $fd_j(\mathbf{X}_j,t)$ and $gd_j(\mathbf{X}_j,t)$ denote the subsystem interactions, $N_d = \sum_{j=1}^{m} n_j$, $\chi = \left(\mathbf{X}_1^T, \ldots, \mathbf{X}_p^T, \ldots, \mathbf{X}_m^T\right)^T \in R^{N_d}$.

For simplicity, we denote $fd_j(\mathbf{X}_j,t)$ as fd_j, etc., in the following.

The global objective of the control system is to design an input vector, $\mathbf{U} = (u_1,u_2,\ldots,u_m)^T \in R^m$, such that the actual output vector, $\mathbf{Y} = (y_1,y_2,\ldots,y_m)^T \in R^m$, will tend to its desired trajectory vector $\mathbf{Y}^d = \left(y_1^d, y_2^d, \ldots, y_m^d\right)^T \in R^m$ when $t \to \infty$.

Because the global system has been decentralized into p interconnected subsystems, the above control objective can be achieved by only considering every subsystem. For instance, for the pth subsystem, it means to design an input $u_p(t)$ such that the tracking error $e_p(t)\ \left(= y_p^d(t) - y_p(t)\right)$ converges uniformly to zero.

The pth subsystem is coupled with other subsystems by the lumped term $d_{p1}(\chi,t)$ that contains the coupling effects from the other subsystems and inner disturbances. When the terms $d_{p1}(\chi,t)$ and $d_{p2}(t)$ are bounded by absolute value, a SFLC controller can be designed to stabilize the pth subsystem. On the other hand, the deterministic part of the disturbances $d_{p1}(\chi,t)$ and $d_{p2}(t)$ can be considered as an unknown deterministic function and it can be approximated by a Fourier integration function and controlled by the proposed FDAC compensator. If the term $d_{p1}(\chi,t)$ is perfectly compensated, each subsystem will be totally decoupled and the decentralized control will work as well as the centralized control. In fact the deterministic part of $d_{p1}(\chi,t)$ within the system bandwidth can be compensated completely by the DNAC controller.

III. SFLC Feedback Control Law

A. Single-Input Fuzzy Logic Control

Consider the pth subsystem of a MIMO nonlinear process defined by (6)–(9), the tracking error and its derivatives can be defined as follows:

$$e_p(t) = y_p(t) - y_p^d(t) = C_p x_p(t) - y_p^d(t) + d_{p2}(t)$$
$$\cdots$$
$$e_p^{(n_p)}(t) = y_p^{(n_p)}(t) - \left(y_p^d\right)^{(n_p)}(t)$$
$$= C_p[f_p(\mathbf{X}_p,t) + g_p(\mathbf{X}_p,t)u_p(t) + d_{p1}(\chi,t)] - \left(y_p^d\right)^{(n_p)}(t) + d_{p2}^{(n_p)}(t). \quad (10)$$

A general sign distance D_p^s can be defined as follows [3], [5]:

$$D_p^s = \frac{e_p^{(n_p-1)} + \lambda_{n_p-1} e_p^{(n_p-2)} + \cdots + \lambda_2 \dot{e}_p + \lambda_1 e_p}{\sqrt{1 + \lambda_{n_p-1}^2 + \cdots + \lambda_2^2 + \lambda_1^2}}. \tag{11}$$

Hence, a fuzzy control rule form for the SFLC of the pth subsystem can be given as follows [5]:

$$R_p^k\text{: If } D_p^s \text{ is } DL_{pk} \text{ then } u_p \text{ is } U_{pk} \tag{12}$$

where DL_{pk} is the linguistic value of a sign distance of the pth subsystem in the kth rule.

From (11), we can see that a general sign distance of a single fuzzy input variable contains information about all process states of the pth subsystem.

Proposition 1: If all the membership functions are assumed to be triangles with equal widths and heights, and their neighboring functions intersect at the level of 0.5, and the product–sum inference and weighting average defuzzification methods are used, then the control output generated by (12) is linear

$$u_p = -K_p^d D_p^s \tag{13}$$

where $K_p^d > 0$ is a constant.

B. Stability Analysis of Closed-Inner-Loop

In this section, we prove the stability of the inner loop when the proposed SFLC is used as the feedback controller.

Theorem 1: If the following conditions are satisfied: 1) $|C_p f_p| \le F_p$; 2) $|C_p d_{p1}(\chi, t)| \le D_{p1}$; 3) $\left|d_{p2}^{(n_p)}\right| \le D_{p2}$; 4) $0 < g_p^{\min} \le g_p \le g_p^{\max}$ and K_p^d satisfies the following inequality:

$$K_p^d \left|D_p^s\right| \ge \left(g_p^{\min}\right)^{-1} \left(F_p + D_{p1} + \sum_{i=1}^{n_p-1} \lambda_i e_p^{(i)} - \left(y_p^d\right)^{(n_p)} + D_{p2} + \eta_p \right), \quad \eta_p \ge 0 \tag{14}$$

then the global SFLC is stable in the sense of Lyapunov.

Proof: We consider a Lyapunov function candidate of the global system as

$$V = \sum_{p=1}^{m} V_p = \frac{1}{2} \sum_{p=1}^{m} \left(D_p^s\right)^2. \tag{15}$$

Then its time derivative becomes

$$\begin{aligned}
\dot{V} &= \sum_{p=1}^{m} \dot{V}_p = \sum_{p=1}^{m} D_p^s \dot{D}_p^s \\
&= \sum_{p=1}^{m} \frac{D_p^s}{\sqrt{\Lambda_p}} \left(e_p^{(n_p)} + \sum_{i=1}^{n_p-1} \lambda_i e_p^{(i)} \right) \\
&= \sum_{p=1}^{m} \frac{D_p^s}{\sqrt{\Lambda_p}} \Bigg\{ C_p \left[f_p - g_p K_p^d \left|D_p^s\right| \operatorname{sign}\left(D_p^s\right) + d_{p1} \right] \\
&\qquad - \left(y_p^d\right)^{(n_p)} + d_{p2}^{(n_p)} + \sum_{i=1}^{n_p-1} \lambda_i e_p^i \Bigg\}
\end{aligned} \tag{16}$$

where $\Lambda_p = \lambda_{n_p-1}^2 + \cdots + \lambda_2^2 + \lambda_1^2 + 1$.

Substituting (14) into (16), we obtain

$$\dot{V} = \sum_{p=1}^{m} \dot{V}_p \le -\sum_{p=1}^{m} \frac{\eta_p}{\sqrt{\Lambda_p}} \left|D_p^s\right| < 0. \tag{17}$$

Therefore, all m subsystems are stable in the sense of Lyapunov and the conclusion is that the global SFLC system is stable.

IV. Design of an Adaptive Compensator in Fourier Space

For convenience, we assume that the controlled system satisfies the following conditions [5].

1) The internal dynamics of every subsystem is stable, i.e., it meets the conditions of Theorem 1 and can be stabilized by output feedback.
2) The desired trajectory $y_p^d(t)$ of the pth subsystem $(p = 1, 2, \ldots, m)$ complies with the actuator's capacity.
3) All subsystems, actuators, and sensors have finite bandwidths.

In process control, the desired trajectory $y_p^d(t)$ is usually given by an operator's demand. It may be a signal that contains full frequency components, e.g., a step function or sloped one. In order to meet condition 2), we can reconstruct a desired trajectory in system bandwidth between 0 and N_2 by

$$\bar{y}_p^d(t) = \sum_{k=0}^{N_2} \left[a_k \cos k\omega t + b_k \sin k\omega t\right] \tag{18}$$

and minimize the following performance index:

$$\begin{aligned}
\text{PI1} &= \min_{a_k, b_k} \int_t^{t+T_m} \left[y_p^d(t) - \bar{y}_p^d(t) \right]^2 dt \\
&= \min_{a_k, b_k} \int_t^{t+T_m} \left[y_p^d(t) - \sum_{k=0}^{N_2} [a_k \cos k\omega t + b_k \sin k\omega t] \right]^2 dt
\end{aligned} \tag{19}$$

where T_m is the smoothing interval which may be whole time or part time taken by the desired trajectory $y_p^d(t)$, ω is base frequency.

From (19), we can obtain the following solutions:

$$a_0 = \frac{\omega}{\pi} \int_t^{t+T_m} y_p^d(t) dt, \quad a_n = \frac{\omega}{\pi} \int_t^{t+T_m} y_p^d(t) \cos k\omega t dt,$$
$$b_n = \frac{\omega}{\pi} \int_t^{t+T_m} y_p^d(t) \sin k\omega t dt.$$

Subject to the above assumptions, and in a discrete domain, the tracking error $e_p(t) \left(= y_p^d(t) - y_p(t)\right)$ of the pth closed-loop subsystem can be expressed as a Fourier integration with finite harmonic terms as follows:

$$\begin{aligned}
e_p(t) = e_p(n\Delta T) &= \Delta\omega \sum_{k=0}^{N_{p2}} \operatorname{Re} e_{pk}(k\Delta\omega) \cos(k\Delta\omega n\Delta T) \\
&\quad + \Delta\omega \sum_{k=0}^{N_{p2}} \operatorname{Im} e_{pk}(k\Delta\omega) \sin(k\Delta\omega n\Delta T) \\
(n &= 1, 2, \ldots, N_1)
\end{aligned} \tag{20}$$

where

$$\operatorname{Re} e_{pk}(k\Delta\omega) = \frac{\Delta T}{\pi} \sum_{n=0}^{N_1-1} e_p(n\Delta T) \cos(k\Delta\omega n\Delta T) \tag{21}$$

$$\operatorname{Im} e_{pk}(k\Delta\omega) = \frac{\Delta T}{\pi} \sum_{n=0}^{N_1-1} e_p(n\Delta T) \sin(k\Delta\omega n\Delta T) \tag{22}$$

where $T_0 = N_1 \Delta T$ is the present time, ΔT is the sample period, $\omega = N_{p2} \Delta\omega$, $\Delta\omega$ is the base angle frequency, and N_{p2} corresponds to the truncating frequency.

It is considered that the tracking error $e_p(t)$ of the pth subsystem is approximated by a summation of $(2N_{p2}+1)$ harmonic sinusoidal and cosine functions as its coordinates or basis

$$1, \cos\omega t, \cos 2\omega t, \ldots, \cos N_{p2}\omega t, \quad \sin\omega t, \sin 2\omega t, \ldots, \sin N_{p2}\omega t. \tag{23}$$

The elements of the basis are orthogonal in the time interval $[0, kT]$, $k \in (0, N_1]$. So the magnitudes (Fourier coefficients) are independent of each other.

The proposed controller of the pth subsystems is the combination of the SFLC controller and the FDAC compensator as in

$$u_{pi}(t) = L_p u_{pi}^{\mathrm{SFLC}} + \hat{u}_{pi}(t) \tag{24}$$

where $\hat{u}_{pi}(t)$ is the output of the FDAC compensator in the ith sample, which is the estimation of input $u_{pi}(t)$, and u_{pi}^{SFLC} is the output of the fuzzy controller in the ith sample, L_p is a positive constant. u_{pi}^{SFLC} is given by

$$\begin{aligned} u_{pi}^{\mathrm{SFLC}} &= f\left(D_p^s\right)\left(K_p^d D_p^s\right)_{pi} \\ &= f\left(D_p^s\right) K_p^d \\ &\times \left(\frac{e_{pi}^{(n_p-1)} + \lambda_{n_p-1} e_{pi}^{(n_p-2)} + \cdots + \lambda_2 \dot{e}_{pi} + \lambda_1 e_{pi}}{\sqrt{1+\lambda_{n_p-1}^2 + \cdots + \lambda_2^2 + \lambda_1^2}}\right) \end{aligned} \tag{25}$$

where e_{pi}, $\dot{e}_{pi}$, and $e_{pi}^{(n_p-1)}$ are the dynamic error, the change rate of the error, and the (n_p-1)th differentiation of the error of the pth subsystem in the ith sample, respectively. $f\left(D_p^s\right)$ is a nonlinear continuous function of D_p^s which does not identically vanish, and can be deduced from (11) and (12).

Equation (24) has the following form in Fourier space:

$$\begin{aligned} u_{pi}(t) =& L_p u_{pi}^{\mathrm{SFLC}} + \hat{u}_{pi}(t) \\ =& \Delta\omega \sum_{k=0}^{N_{p2}} L_p p_{pik} \cos(k\Delta\omega n \Delta T) \\ &+ \Delta\omega \sum_{k=0}^{N_{p2}} L_p q_{pik} \sin(k\Delta\omega n \Delta T) \\ &+ \Delta\omega \sum_{k=0}^{N_{p2}} \hat{a}_{pik} \cos(k\Delta\omega n \Delta T) \\ &+ \Delta\omega \sum_{k=0}^{N_{p2}} \hat{b}_{pik} \sin(k\Delta\omega n \Delta T) \\ =& \Delta\omega \sum_{k=0}^{N_{p2}} (a_{pik} \cos(k\Delta\omega n \Delta T) \\ &+ b_{pik} \sin(k\Delta\omega n \Delta T)) \end{aligned} \tag{26}$$

where

$$p_{pik} = \frac{\Delta T}{\pi} \sum_{n=0}^{N_1-1} u_{pi}^{\mathrm{SFLC}} \cos(k\Delta\omega n \Delta T) \tag{27}$$

$$q_{pik} = \frac{\Delta T}{\pi} \sum_{n=0}^{N_1-1} u_{pi}^{\mathrm{SFLC}} \sin(k\Delta\omega n \Delta T). \tag{28}$$

Thus, the problem of obtaining $u_{pi}(t)$ becomes one of finding the suitable harmonic magnitudes $\hat{a}_{pik}$ and $\hat{b}_{pik}$.

Intuitively, if we could find an update law to force $\hat{a}_{pik}$ and $\hat{b}_{pik}$ to tend to a_{pik} and b_{pik} as $t \to \infty$, then $\hat{u}_{pi}(t)$ will tend to $u_{pi}(t)$. Moreover, u_{pi}^{SFLC} will then approach zero and the output error $e_{pi}(t)$ will be asymptotically convergent from (25).

By using the Lyapunove stability principle the following adaptive compensation control law of the pth subsystem in the ith sample can be deduced

$$\begin{aligned} \hat{a}_{pik} =& \hat{a}_{p(i-1)k} + \Delta a_{p(i-1)k} + \gamma_p p_{p(i-1)k} \\ & (k = 1, 2, \ldots, N_{p2}) \end{aligned} \tag{29}$$

$$\begin{aligned} \hat{b}_{pik} =& \hat{b}_{p(i-1)k} + \Delta b_{p(i-1)k} + \gamma_p q_{p(i-1)k} \\ & (k = 1, 2, \ldots, N_{p2}) \end{aligned} \tag{30}$$

$$\begin{aligned} \Delta a_{p(i-1)k} =& a_{p(i-1)k} - a_{p(i-2)k} \\ & (k = 1, 2, \ldots, N_{p2}) \end{aligned} \tag{31}$$

$$\begin{aligned} \Delta b_{p(i-1)k} =& b_{p(i-1)k} - b_{p(i-2)k} \\ & (k = 1, 2, \ldots, N_{p2}). \end{aligned} \tag{32}$$

In (29)–(32) γ_p is an adaptive gain and it is a positive constant, the initial conditions are $\hat{a}_{p0k} = \hat{b}_{p0k} = a_{p0k} = b_{p0k} = 0$.

Here we define three vectors

$$\begin{aligned} U_{pi} =& [\,a_{pi0} \quad a_{pi1} \quad \ldots \quad a_{piN_{p2}} \quad b_{pi1} \quad b_{pi2} \quad \ldots \quad b_{piN_{p2}}\,] \\ =& [\,u_{pi1} \quad u_{pi2} \quad \ldots \quad u_{pi(2N_{p2}+1)}\,]; \end{aligned} \tag{33}$$

$$\begin{aligned} \hat{U}_{pi} =& [\,\hat{a}_{pi0} \quad \hat{a}_{pi1} \quad \ldots \quad \hat{a}_{piN_{p2}} \quad \hat{b}_{pi1} \quad \hat{b}_{pi2} \quad \ldots \quad \hat{b}_{piN_{p2}}\,] \\ =& [\,\hat{u}_{pi1} \quad \hat{u}_{pi2} \quad \ldots \quad \hat{u}_{pi(2N_{p2}+1)}\,]; \end{aligned} \tag{34}$$

$$\begin{aligned} O_{pi} =& [\,p_{pi0} \quad p_{pi1} \quad \ldots \quad p_{piN_{p2}} \quad q_{pi1} \quad q_{pi2} \quad \ldots \quad q_{piN_{p2}}\,] \\ & [\,o_{pi1} \quad o_{pi2} \quad \ldots \quad o_{pi(2N_{p2}+1)}\,]. \end{aligned} \tag{35}$$

Let us denote

$$\begin{aligned} \Delta o_{pik} =& o_{pik} - o_{p(i-1)k} \\ \Delta u_{pik} =& u_{pik} - u_{p(i-1)k} \\ \Delta u_{p(i-1)k} =& u_{p(i-1)k} - u_{p(i-2)k} \\ \Delta \hat{u}_{pik} =& \hat{u}_{pik} - \hat{u}_{p(i-1)k} \\ \Delta^2 u_{pik} =& \Delta u_{pik} - \Delta u_{p(i-1)k} \\ \beta_{p1} =& \frac{\gamma_p}{L_p}. \end{aligned}$$

Theorem 2: The global closed-loop system (6) and (7) is asymptotically stable if the compensation controller (26) is updated according to the recursive update law (29) and (30), provided that $L_p > \max_{i,k} \left|(\Delta^2 u_{pik}/\Delta o_{pik})\right| 1/(1-\beta_{p1})$

Proof: If all the m subsystems are stable, then the global closed-loop system is stable. Next, we first prove the stability of the pth subsystem.

From (26), we have

$$L_p \Delta o_{pik} = \Delta u_{pik} - \Delta \hat{u}_{pik}. \tag{36}$$

Equations (29) and (30) can be represented as

$$\Delta \hat{u}_{pik} = \Delta u_{p(i-1)k} + \gamma_p o_{p(i-1)k} \quad (i \geq 1). \tag{37}$$

Substituting (37) into (36), we obtain

$$\Delta u_{pik} - \Delta u_{p(i-1)k} = \gamma_p o_{p(i-1)k} + L_p \Delta o_{pik}. \tag{38}$$

When $\Delta o_{pik} \neq 0$, the above equation can be rewritten as

$$\gamma_p o_{p(i-1)k} + \left(1 - \frac{\Delta^2 u_{pik}}{L_p \Delta o_{pik}}\right) L_p \Delta o_{pik} = 0. \tag{39}$$

The above equation can be expressed as follows:

$$\frac{o_{pik}}{o_{p(i-1)k}} = 1 - \frac{\frac{\gamma_p}{L_p}}{1 - \frac{\Delta^2 u_{pik}}{L_p \Delta o_{pik}}} = 1 - \frac{\beta_{p1}}{1 - \frac{\Delta^2 u_{pik}}{L_p \Delta o_{pik}}}. \quad (40)$$

In order to ensure the error of the system converges to zero, it is necessary that the following holds:

$$0 < \frac{\beta_{p1}}{1 - \frac{\Delta^2 u_{pik}}{L_p \Delta o_{pik}}} < 2. \quad (41)$$

If the learning gain is selected from the range $0 < \beta_{p1} < 1$ and the closed-loop system satisfies

$$L_p > \max_{i,\,k} \left| \frac{\Delta^2 u_{pik}}{\Delta o_{pik}} \right| \frac{1}{1 - \beta_{p1}} \quad (42)$$

then we have

$$\left| \frac{o_{pik}}{o_{p(i-1)k}} \right| < \alpha_p < 1. \quad (43)$$

Thus, we can obtain

$$|o_{pik}| < \alpha_p \left|o_{p(i-1)k}\right| < \alpha_p^2 \left|o_{p(i-2)k}\right| < \cdots < \alpha_p^i \left|o_{p0k}\right|. \quad (44)$$

Since the initial value of o_{p0k} is finite, as $i \to \infty$, we have $o_{pik} \to 0$.

In Fourier space, the above analysis holds for all harmonic components. This implies that in the time-domain the following exists:

$$K_p^d D_p^s = 0. \quad (45)$$

Since K_p^d is a constant, (45) means $D_p^s = S_p/\sqrt{\Lambda} = 0$. Because $S_p (= e_p^{(n_p-1)} + \ldots + \lambda_l e_p)$ is a stable hyperplane, then $e_p = 0,\ \dot{e}_p = 0, \ldots, e_p^{(n-1)} = 0$, as $i \to \infty$.

Because every tracking error in any subsystem meets

$$\lim_{t\to\infty} e_p = 0 \Rightarrow \lim_{t\to\infty} \left(y_p - y_p^d\right) = 0 \Rightarrow \lim_{t\to\infty} y_p = \lim_{t\to\infty} y_p^d \quad (46)$$

we conclude that the global system (6) and (7) is stable. □

Remark 1: Most real systems can be characterized as a low-pass filter because their bandwidth is much lower than the sampling frequency. Based on this reason, the Fourier integration of $\hat{u}_p$ in the pth subsystem is truncated into summations from 0 to N_{p2} instead of 0 to ∞.

Remark 2: If the controlled system meets condition 1) and 3), but the desired trajectory exceeds the actuator's capacity at some limited intervals during operation (e.g., at the beginning period of the whole operation), then because the FDAC method integrates the tracking error sequence, it can gradually remove all the frequency components in system bandwidth and the tracking error still converges uniformly to zero.

V. Simulation Study on a HVAC System

The system parameters in the HVAC model expressed by (1)–(5) are the same as that given by [1], i.e., $\rho = 0.074$ lb/ft^3 $(1.19K_g\ /\text{m}^3)$, $C_p = 0.24$ Btu/lb $\cdot^\circ$ F $(1.005K_j/K_g \cdot^\circ \text{C})$, $f_{\text{ref}} = 17\,000$ cfm, $f_{0\text{ref}} = 4250$ cfm, $t_f = 24$ hours, $T_{0w} = 72\,^\circ$F, $T_{2w} = 55\,^\circ$F, $T_{3w} = 60\,^\circ$F, $T_{2\text{ref}} = 55\,^\circ$F, $T_{3\text{ref}} = 71\,^\circ$F, $W_s = 0.0070$ lb/lb, $W_{3\text{ref}} = 0.0088$ lb/lb, $V_e = 60.75$ ft^3, $V_s = 58\,464$ ft^3, $h_v = 1087.1$ Btu/lbm, $h_w = 23.0$ Btu/lbm.

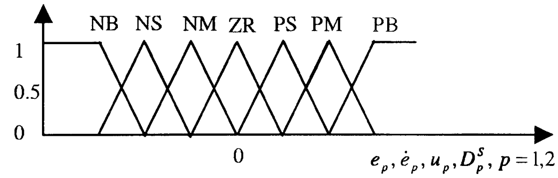

Fig. 2. Fuzzy sets for the simulation of HVAC.

TABLE I
Comparison Results

references		[5]	[1]	Our methods	
methods		FLC	NCB	SFLC	DNAC
performances	Setting time (min)	13	12	8	5.4
	PER defined by (57)	1957	2016	548	53.5

Equilibrium conditions of the HVAC system are set as $T_3^e = 71\,^\circ$F, $W_3^e = 0.0092$ lb/lb, $T_2^e = 55\,^\circ$F, $T_0^e = 85\,^\circ$F, $W_0^e = 0.018$ lb/lb, $M_0^e = 166.06$ lb/hr, $u_1^e = 17\,000$ cfm, $u_2^e = 58$ gpm, $Q_0^e = 289\,897.52$, $W_s^e = 0.0070$ lb/lb.

In the following simulation two cases are considered.

A. With the Ambient Temperature T_0 Step-Changing

The switching line of the sliding mode surface is chosen to be

$$S_1: \dot{e}_1 + 1.8e_1 = 0 \quad (47)$$
$$S_2: \dot{e}_2 + 2.1e_2 = 0 \quad (48)$$

and the performance index is defined as

$$\text{PER} = \int_0^T [k_1 |e_1| + k_2 |e_2|] dt \quad (49)$$

where

$$e_1 = \int_0^t W_3 dt - \int_0^t W_{3\text{ref}} dt, \quad e_2 = \int_0^t T_3 dt - \int_0^t T_{3\text{ref}} dt,$$
$$\dot{e}_1 = W_3 - W_{3\text{ref}}, \quad \dot{e}_2 = T_3 - T_{3\text{ref}}, \quad k_1 = k_2 = 1.5.$$

Fig. 2 presents the fuzzy sets for error, change rate of error, control input, and sign distance.

Choose $N_{12} = 5$, $N_{22} = 2$, sampling period $= 0.000\,66$ min, $\gamma_1 = 0.4$, $\gamma_2 = 0.4$.

As a comparison, the nonlinear control (NCB) proposed by [1] is applied to the HVAC system also. Because no established procedure for tuning PI controller parameters for a nonlinear control problem like this HVAC exists, the PI controller is excluded from this case study. We suppose that the system is acted upon by norminal thermal loads, ambient temperature T_0 was set to 85 °F (equilibrium value) initially, and it was changed to 87 °F. Table I presents the concrete comparison results and we see that, when the ambient temperature T_0 *step-changing*, SFLC has obvious stable errors, NCB has a large dynamic error and a slow dynamic response. However DNAC has the least stable errors and the fastest dynamic responses among the four methods. We can thus see that the performance of this DNAC controller is the best among the four schemes.

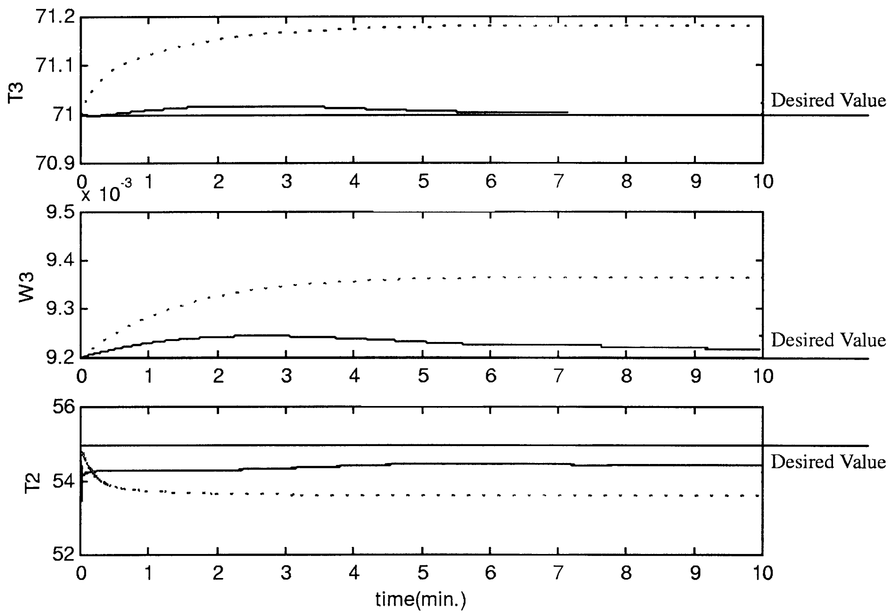

Fig. 3. Comparison curves between the two methods in the face of thermal loads above design value. Dotted line: the system outputs with the SFLC controller; solid line: the system outputs with DNAC.

B. When Subjected to Thermal Loads Above the Design Value With Disturbances

Unfortunately, HVAC systems are rarely acted upon by design thermal loads. Fig. 3 shows the performance of the system when subjected to thermal loads above the design value and with disturbances. The value of the loads for this simulations are $Q_0 = 350\,000$ Btu/hr and $M_0 = 196$ lb/lb.

The dynamics of the disturbances are supposed as

$$F_{p1} = C_1(t) + C_2(t - t_1) + C_3 \mathrm{rand}_1 \sin(C_4 t) + C_5 e^{-C_6(t - C_7 - C_8 \mathrm{rand}_2)(t - C_7 - C_8 \mathrm{rand}_2)} \quad (p = 1, 2) \tag{50}$$

$$d_{p2} = C_9 + C_{10} e^{-C_{11} t^2} \quad (p = 1, 2). \tag{51}$$

In (50), $C_1(t)$ and $C_2(t)$ are two step perturbations, and rand_1 and rand_2 are two independent random real numbers between 0 and 1. Here $C_1 = 0.5, C_2 = 0.01, C_3 = -0.2, C_4 = 3.14, C_5 = 3, C_6 = 0.008$, $C_7 = 45$, $C_8 = 8$, $t_1 = 0.5$ min, $C_9 = 0.001$, $C_{10} = 30\,000$, $C_{11} = 0.05$.

From Fig. 3 we can see that this DNAC controller for the HVAC process has a smaller overshoot, shorter settling time TS, and better performance PER than the SFLC does, though it suffers from a variety of random noises and time-variant lasting uncertain disturbances. In Fig. 3, when the DNAC controller is used the tracking errors of T_3 and W_3 converge uniformly to zero respectively, but T_2 does not. This is because T_2 is not controlled at all.

Based on the above simulation results, it is evident that the proposed scheme is an effective and promising approach to process control, providing robust control without abrupt control actions.

VI. Conclusion

Since the FDAC compensator is designed in Fourier space, it can automatically tune the compensator not only toward a suitable magnitude but also toward a suitable phase. As a result, it can easily cope with the system's time delay and time-variant lasting uncertain disturbances.

The DNAC control scheme has a higher precision, smaller overshoot, shorter settling time TS, and better performance PER, than the FLC, SFLC, and NPC, under random noise and time-variant lasting uncertain disturbances. These aspects of the control system performance are very important to process control problems.

References

[1] A. S. Betzaida and V. R. Miguel, "Nonlinear control of a heating, ventilating, and air conditioning system with thermal load estimation," *IEEE Trans. Contr. Syst. Technol.*, vol. 7, pp. 56–63, Jan. 1999.

[2] M. Bodson, A. Sacks, and P. Khosla, "Harmonic generation in adaptive feedforward cancellation schemes," *IEEE Trans. Automat. Contr.*, vol. 39, pp. 1939–1944, Sept. 1994.

[3] B. J. Choi, S. Kwak, and B. Kim, "Design of a single-input fuzzy logic controller and its properties," *Fuzzy Sets Syst.*, vol. 106, pp. 299–308, Feb. 1999.

[4] Z. Huaguang, L. Cai, and Z. Bien, "Fuzzy basis function vector based multivariable adaptive controller for nonlinear systems," *IEEE Trans. Syst., Man, Cybern. B*, vol. 30, pp. 210–217, Feb. 2000.

[5] Z. Huaguang and L. Cai, "Nonlinear adaptive control using the Fourier integral and is application to CSTR systems," *Syst., Man, Cybern. B*, vol. 32, pp. 367–373, June 2002.

[6] M. S. Imbabi, "Computer validation of scale model tests for building energy simulation," *Int. J. Energy Res.*, vol. 14, pp. 727–736, May 1990.

[7] G. Ray and C. S. Rani, "Stabilizing decentralized robust controllers of interconnected uncertain power systems based on the Hessenberg form: Simulated results," *Int. J. Syst. Sci.*, vol. 32, pp. 387–399, Mar. 2001.

[8] R. Shoureshi, "Intelligent control systems: Are they are real," *J. Dynamic Syst., Measur. Contr.*, vol. 115, pp. 15–19, Jan. 1993.

[9] C. Wen and Y. C. Soh, "Decentralized model reference adaptive control without restriction on subsytem relative degree," *IEEE Trans. Automat. Contr.*, vol. 44, pp. 1464–1468, July 1999.

[10] M. Yaqub and S. M. Zubair, "Capacity control for refrigeration and air-conditioning systems: A comparative study," *Int. J. Energy Res. Tech.*, vol. 123, pp. 92–99, Apr. 2001.